OMTO, Volume *12*

Supplemental Information

Two-Dimensional Regulation of CAR-T Cell Therapy with Orthogonal Switches

MyLinh T. Duong, Matthew R. Collinson-Pautz, Eva Morschl, An Lu, Slawomir P. Szymanski, Ming Zhang, Mary E. Brandt, Wei-Chun Chang, Kelly L. Sharp, Steven M. Toler, Kevin M. Slawin, Aaron E. Foster, David M. Spencer, and J. Henri Bayle

Figure S1

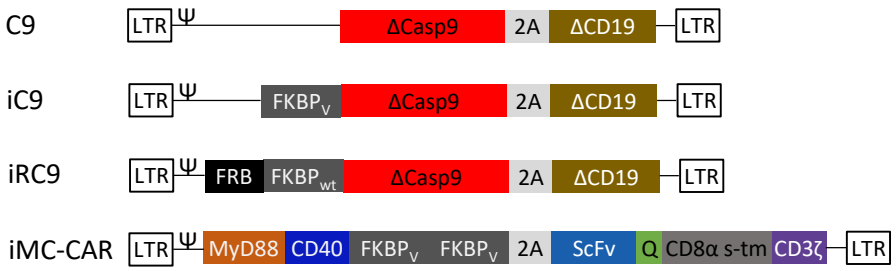

ACTIVATION SWITCH

- "On demand" co-stimulation via rimiducid administration enhances cell proliferation and activation.
- Full activation and tumor cell killing requires a second, target-specific CD3ζ signal.

APOPTOTIC SWITCH

- Rapid and efficient clearance of T cells follows rapamycin administration.
- Titration of rapamycin allows partial T cell elimination, preserving CAR-T function.

Figure S1. Schematic of γ-retroviral vectors encoding C9, iC9, iRC9, and iMC-CAR. Constructs consist of 5' and 3' long terminal repeats (LTRs), ψ packaging signal, truncated caspase-9, *Thosea asigna virus* 2A cotranslational cleavage, truncated CD19, FKBP12 wild-type or FKBP12v36, FRB, MyD88, CD40, single-chain variable fragment (heavy and light) specific for the indicated antigens, CD34 QBEnd10 marker, CD8 stalk and transmembrane domain, and the intracellular signaling domains from TCR-ζ.

1. Kim, J.H., *et al.* High cleavage efficiency of a 2A peptide derived from porcine teschovirus-1 in human cell lines, zebrafish and mice. *PLoS One* **6**, e18556 (2011).

Figure S2

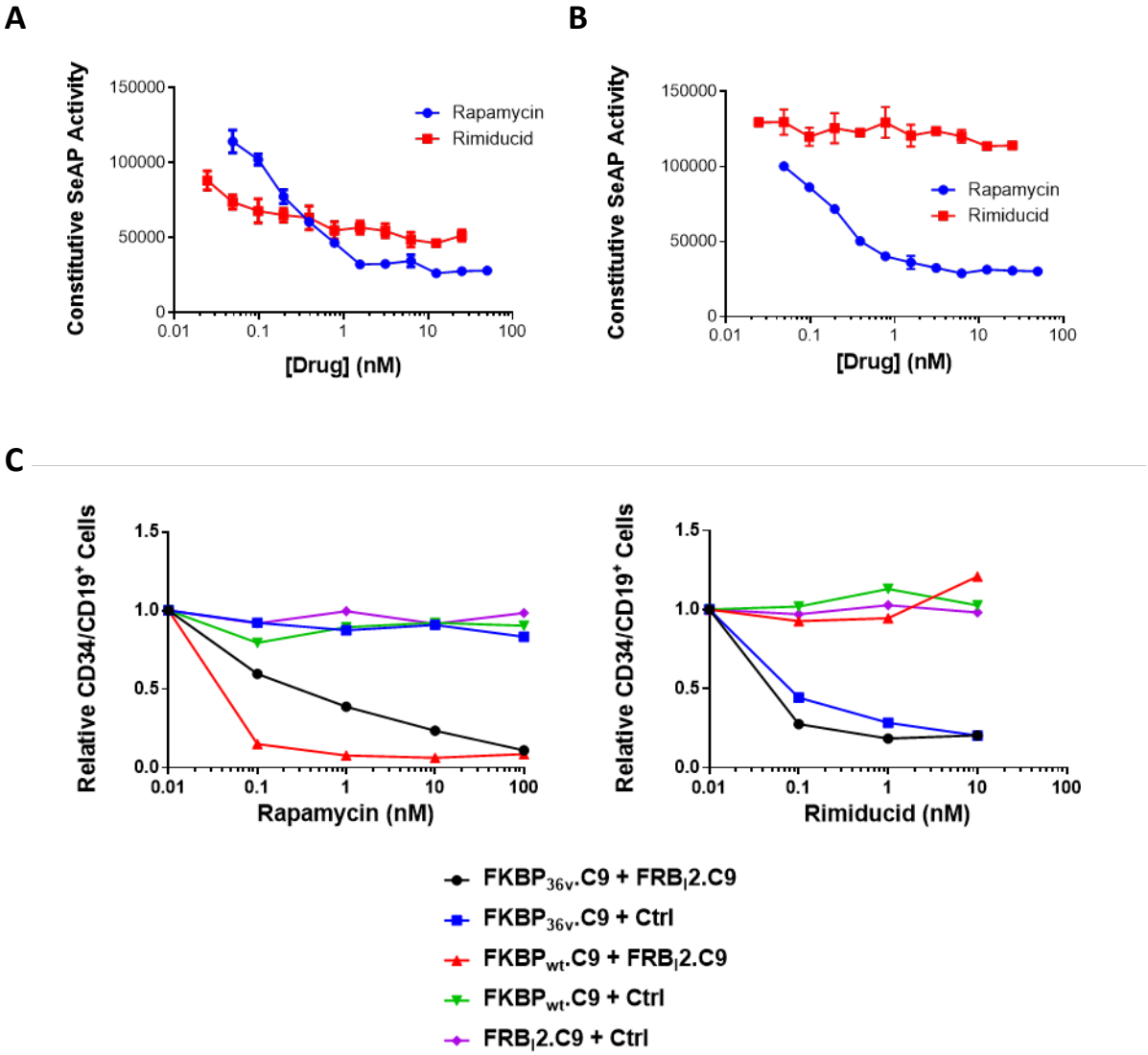

Figure S2. Induction of a proapoptotic switch with Rap. **(a)** Fusion of the FRB domain and truncated Caspase-9 lacking the CARD domain (FRB-C9) and an FKBPv36-C9 fusion were coexpressed in HEK293 cells with a constitutively active Secreted Alkaline Phosphatase (SeAP) reporter. Induction of apoptosis with increasing doses of Rap caused apoptosis and reduction of reporter activity. Rim dosage causes homodimerization of Fv-C9 and induction of apoptosis. **(b)** Coexpression of FRB-C9 with FKBPwt-C9 permits apoptosis only with Rap but not with Rim. **(c)** Primary human Peripheral Blood Mononuclear Cells (PBMCs) were transduced with γ-retroviruses encoding the indicated protein fusions marked with epitopes to CD34 (Qbend10) and ΔCD19. Expression of FRB-C9 and Fv-C9 or Fwt-C9 caused ablation of the cotransduced population with increasing Rap dosage while only the Fv-C9 population was Rim-sensitive regardless of FRB-C9.

Figure S3

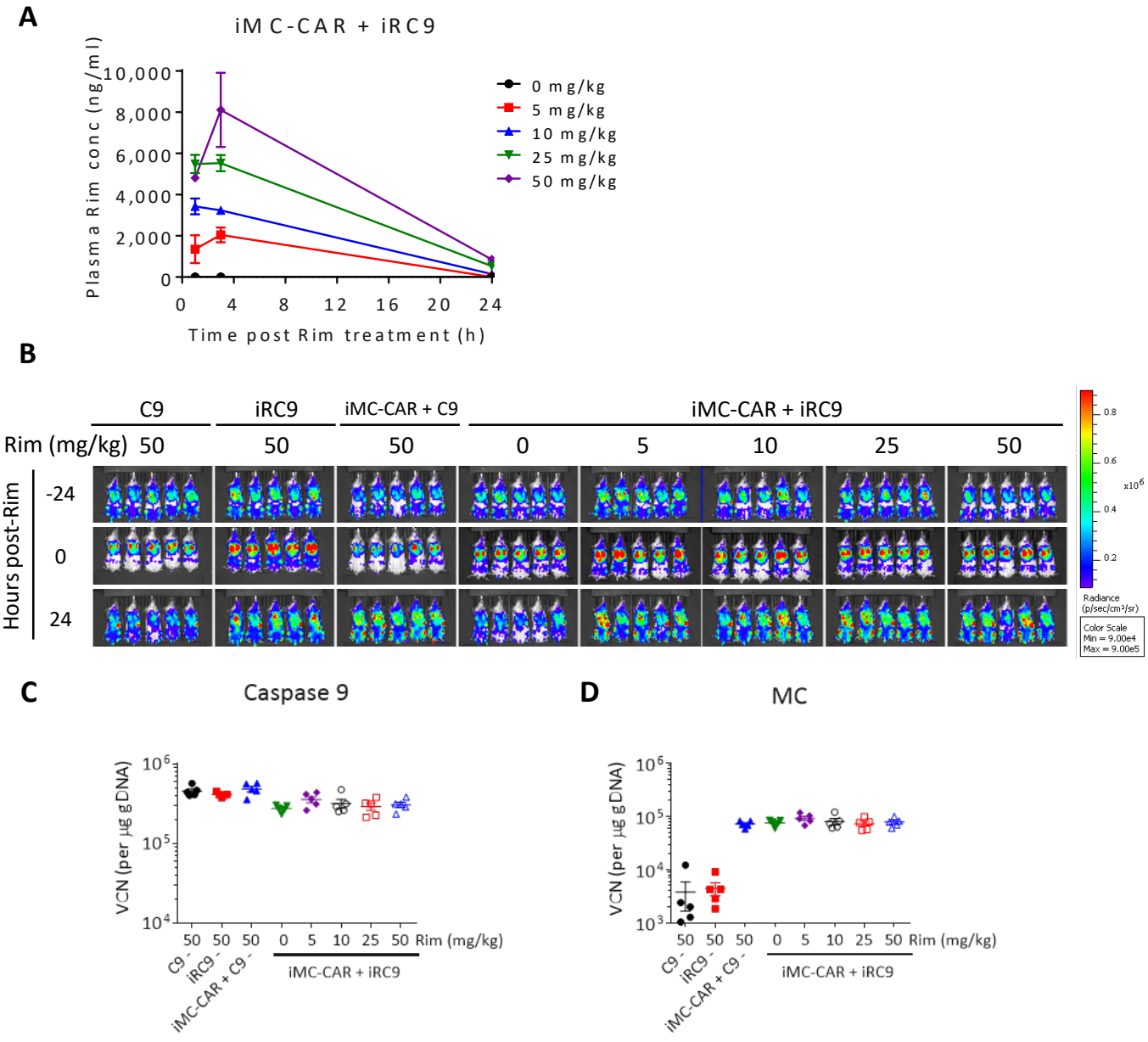

Figure S3. Absence of crosstalk between the Rim-activated iMC switch and the proapoptotic iRC9 safety switch. To determine if high Rim levels can activate iRC9 *in vivo*, 1x10^7 CD19-selected T cells transduced to express uninducible C9 or iRC9, with or without iMC, were injected i.v. into NSG mice 24 hrs before Rim (0, 5, 10, 25, or 50 mg/kg, i.p.) treatment. **(a)** To measure Rim pharmacokinetics, plasma was collected at 1, 3 and 24 hrs post-Rim administration and analyzed via liquid chromatography - mass spectrometry. **(b)** T cell BLI was assessed at -24, 0, and 24 hrs post-Rim administration. **(c & d)** Spleens were isolated 48 hrs post-Rim and DS CAR-T levels were analyzed for C9 **(c)** and MC **(d)** levels by Vector Copy Number (VCN) assay in gDNA.

Figure S4

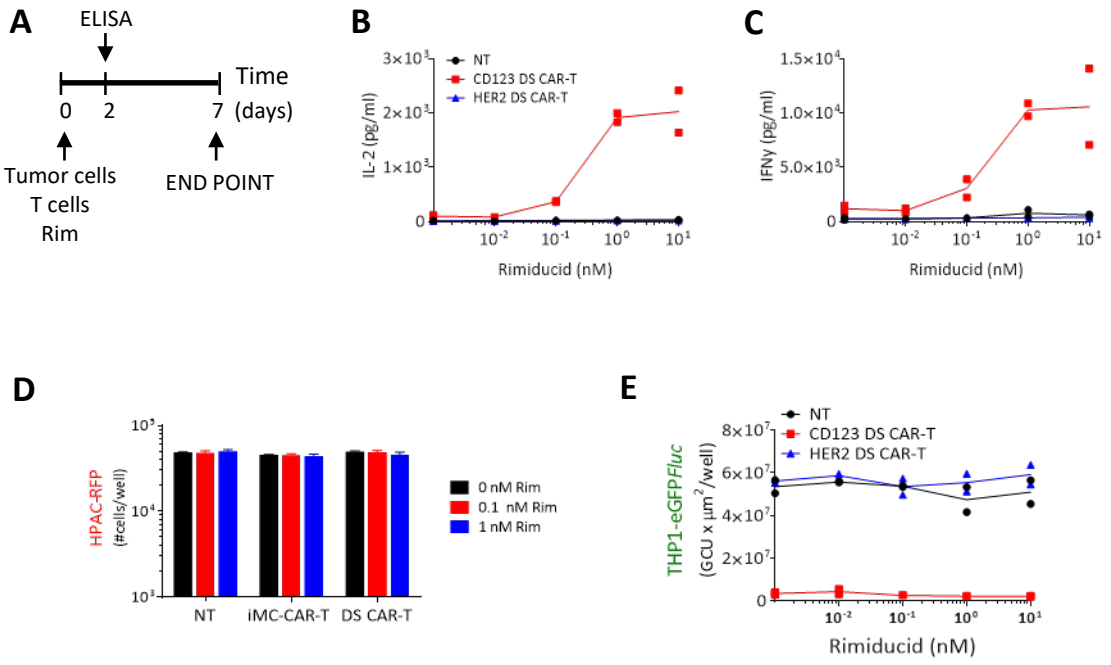

Figure S4. Efficacy and specificity CD123 DS CAR-T cells *in vitro.* Activated T cells were transduced with retrovirus encoding the CD123 or HER2 iMC-CAR vector ± iRC9 vector. **(a)** To assess anti-tumour activity *in vitro*, T cells were cocultured at 1:10 E:T ratio with THP1-GFP or HPAC-RFP cells in the presence of Rim and monitored via IncuCyte for tumour and T cell growth kinetics. **(b, c)** Two days post-seeding, culture supernatants from a duplicate plate of THP1-GFP cocultures were analyzed for IL-2 and IFN-γ production by ELISA. **(d, e)** On day 7, total red fluorescent HPAC-RFP cells ($CD123^-$) **(d)** and green fluorescence intensity (GCU x μm^2/well) of THP1-GFP ($CD123^+$) **(e)** per well were analyzed via IncuCyte basic analyzer software.

Figure S5

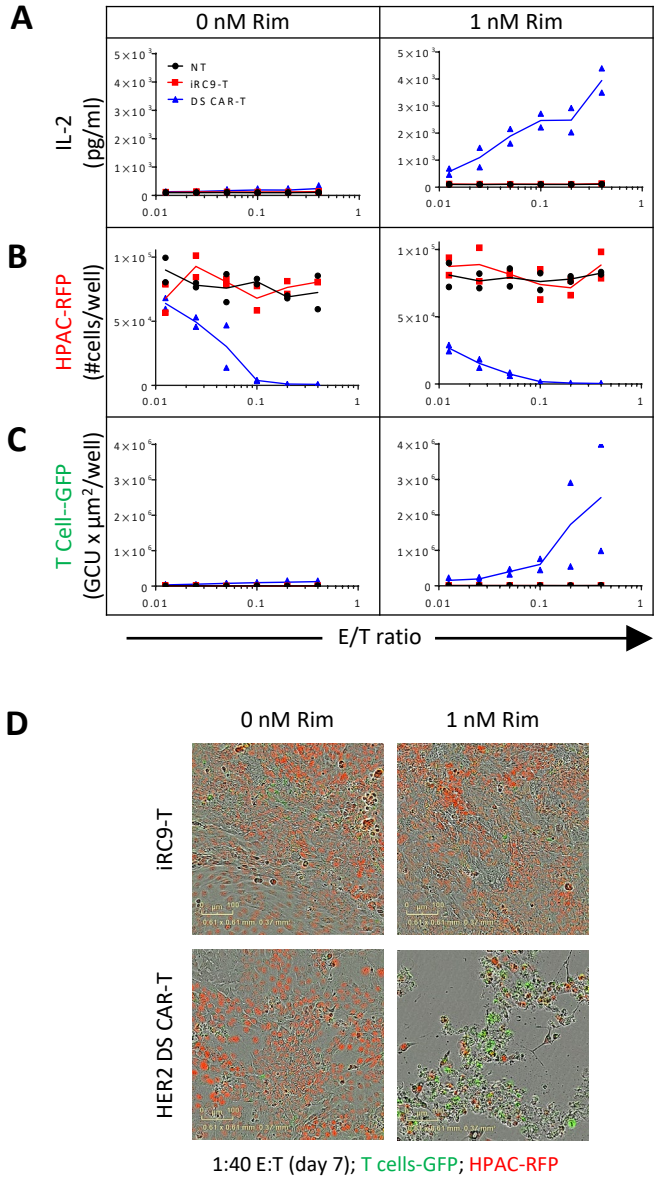

Figure S5. Activation of the iMC switch enhances tumour killing and HER2 DS CAR-T cell proliferation *in vitro*. Activated PBMCs from 2 donors were transduced with retroviruses encoding a HER2 iMC-CAR-T vector ± iRC9 vector. **(a-d)** To assess antitumour activity *in vitro*, T cells (co-labeled with GFP) were co-cultured at various E:T ratios with the pancreatic tumour target cell line HPAC-RFP ± Rim. **(a)** Two days post-seeding, culture supernatants from a duplicate plate were analyzed for IL-2 production by ELISA. **(b & c)** On day 7, red HPAC-RFP cells per well **(b)** and total green fluorescence intensity (GCU x µm^2/well) of T cell-GFP per well **(c)** were analyzed using IncuCyte basic analyzer software. **(d)** Representative images from the co-culture containing HPAC-RFP and iRC9 or HER2 DS CAR-T cells-GFP on day 7 in the presence or absence of Rim.

Figure S6

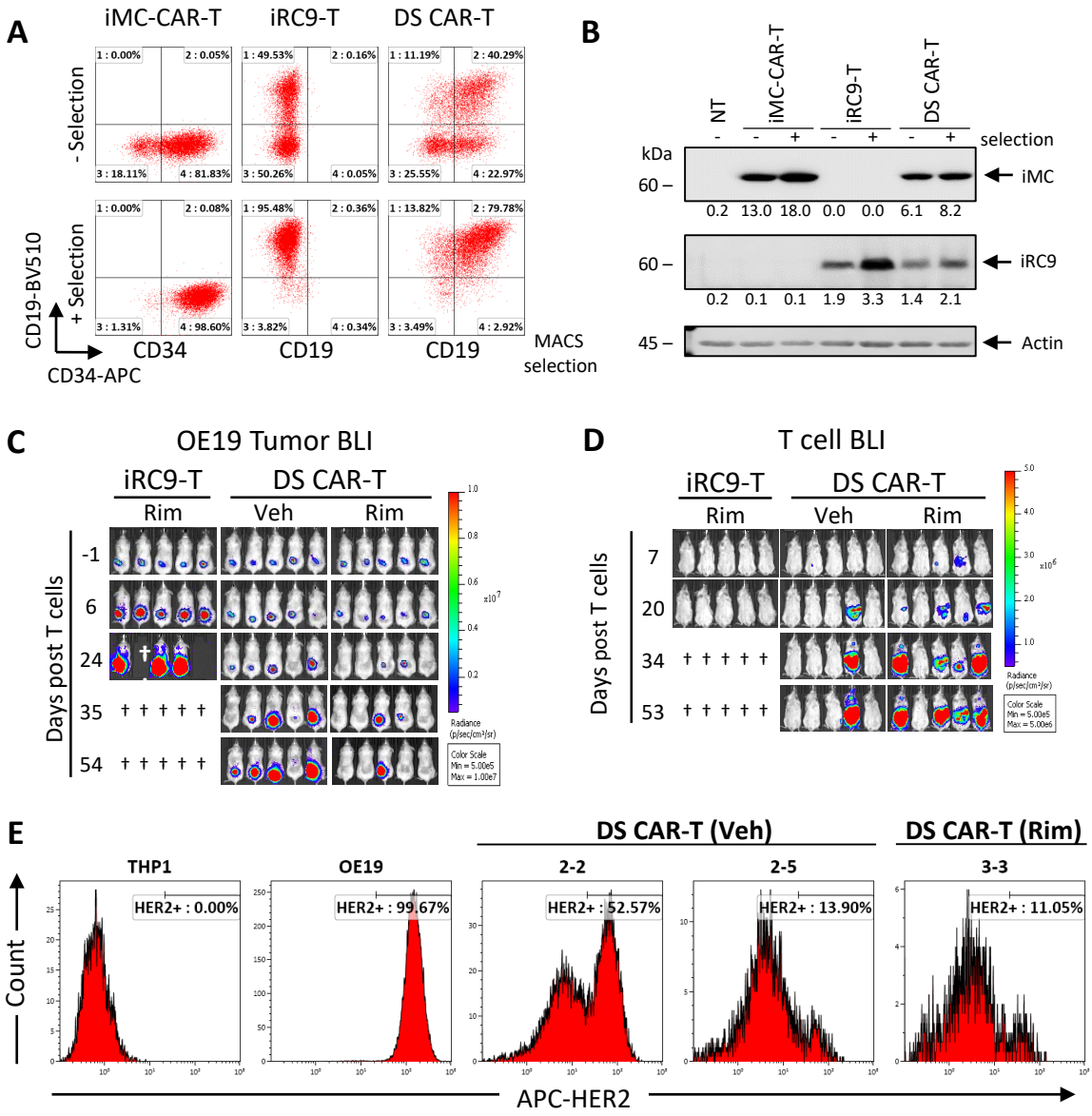

Figure S6. iMC activation enhances HER2^{+} tumor killing and HER2 DS CAR-T cell proliferation. **(A)** PBMCs from 2 donors were activated and co-transduced with HER2 iMC-CAR-T ± iRC9 vectors. Transduction levels were determined by flow cytometry staining for hCD3, hCD19, and hCD34. **(B)** Five days after selection, Western blot analysis was performed to measure iMC (anti-MyD88 antibody), iRC9 (anti-caspase9 antibody), and β-actin protein levels. **(C-E)** NSG mice were engrafted s.c. with $2x10^6$ OE19-eGFPFluc cells for 4 days followed by i.v. injection of $2.5x10^6$ CD19-selected DS CAR-T cells (co-labeled with ONLRluc). Rimiducid (1 mg/kg) or placebo were given i.p. on day 0 and weekly thereafter. **(C)** OE19-eGFPFluc growth was measured by IVIS BLI with D-luciferin substrate. **(D)** T cell expansion was measured by IVIS BLI with coelenterazine substrate. **(E)** On day 54 tumors were excised and dissociated. HER2 expression was compared with the parent OE19 cell line and HER2 negative THP1 cells. CAR-specific antigen was reduced in the tumor of mouse 3-3 treated with rimiducid and mouse 2-5 which was not rimiducid treated.